**248/08/YA**

# Swimbladder condition and target strength of myctophid fish in the temperate zone of the Northwest Pacific

Hiroki Yasuma, Kouichi Sawada, Yoshimi Takao, Kazushi Miyashita, and Ichiro Aoki

Yasuma, H., Sawada, K., Takao, Y., Miyashita, K., and Aoki, I. 2010. Swimbladdder condition and target strength of myctophid fish in the temperate zone of the Northwest Pacific. – ICES Journal of Marine Science, 67: 000–000.

We report theoretical values of the target strength (*TS*) of four myctophid fish (*Ceratoscopelus warmingii*, *Myctophum asperum*, *Diaphus garmani*, and *D. chrysorhynchus*) based on morphometry of the swimbladder. None of the *D. chrysorhynchus* had an inflated swimbladder, but the other species had both inflated and non-inflated swimbladders, depending on body size. The relationships between swimbladder and body length showed that once gas production started the swimbladders grew faster than the rest of the body (positive allometric growth). However, *M. asperum* showed regression of the swimbladder after positive allometric growth, so larger specimens had non-inflated swimbladders. Based on the measurements of swimbladder and body length, the theoretical *TS* values at 38 and 120 kHz were calculated using existing sound-scattering models. In fish with inflated swimbladders, *TS* values were relatively low (<–67 dB, reduced $TS_{cm}$) at both frequencies. Regression slopes on *TS*–body length (log) plots were >20, suggesting that their scattering cross sections were not proportional to the square of the body length. In contrast, the *TS* values of *M. asperum* decreased with growth in large fish (60–80 mm long) through swimbladder regression. Scattering cross sections of fish without swimbladders were not proportional to the square of the body length over the whole size range. They increased rapidly relative to growth, especially when $L/\lambda < 2$.



**Keywords**: acoustic resonance, myctophid fish, swimbladder allometry, theoretical target strength.

Received 19 December 2008; accepted 25 May 2009.

*H. Yasuma and K. Miyashita: Field Science Centre for the Northern Biosphere, Hokkaido University, 3-1-1 Minato, Hakodate, Hokkaido 041-8611, Japan. Y. Takao and K. Sawada: National Research Institute of Fisheries Engineering, Ebidai, Hasaki, Kashima, Ibaraki 314-0408, Japan. I. Aoki: Graduate school of Agricultural and Life Science, University of Tokyo, 1-1-1 Yayoi, Bunkyo, Tokyo*

*113-8657, Japan. Correspondence to H. Yasuma, tel: +81 138 408817; fax: +81 138 408817; e-mail: ANB52615@nifty.com*

## Introduction

Myctophids are the dominant mesopelagic fish taxon in temperate and subtropical waters of the Northwest Pacific, and reliable biomass estimates are needed. The use of acoustic methods is thought to be the best way to do this (Gjøsaeter and Kawaguchi, 1980)

Acoustic surveys measure the scattered sound in the water column, so we need to know the target strength (*TS*) of individual fish to convert the measured backscattered energy into an estimate of fish biomass. The paradigm that the acoustic cross section is proportional to the square of body length and the "20 log length" relationship is often used to estimate fish *TS* over a range of sizes (Foote, 1979; MacLennan and Simmonds, 1992), but some fish groups, especially deep-water fish, do not follow the rule. This is because the growth of the main scattering structure (the swimbladder, in many cases) does not grow in proportion to the rest of the body (McClatchie *et al*., 2003; Yasuma *et al*., 2003). Moreover, myctophid swimbladder condition varies both among and within species, so there is huge variation in *TS* (Capen, 1967; Neighbors and Nafpaktitis, 1982; Yasuma *et al*., 2003). It is important to know how this condition changes with growth in each species. The confidence intervals for even a relative biomass assessment would need to be quite wide until we understand the relationship between swimbladder condition and *TS* better.

Many theoretical models have been developed to estimate the *TS* of marine organisms (Horne and Clay, 1998). Theoretical models approximate the main source of soundscatter, i.e. the swimbladder (or the body of fish without swimbladders), as a geometric configuration. The use of these models has several merits; they can reduce the number of experimental measurements, estimate the backscatter pattern relative to fish orientation, and estimate the *TS* of small-bodied fish with reduced or no swimbladders, or deep-sea fish, which have a very weak soundscatter and for which there are no *in situ* measurements. Using 14 species of myctophids around Japan, Yasuma (2004) computed the pitch-angle shifts of *TS* values using theoretical models after making morphological measurements of the swimbladder and the fish body, and compared these results with experimental measurements conducted in a tank. The study showed that the *TS* values and the shifts computed by the vacant prorate-spheroid model (PSM; Furusawa, 1988) closely matched the results of experimental measurements for fish with a well-inflated swimbladder. The computed results using the liquid deformed-cylinder model (DCM; Ye *et al*., 1997) closely matched the results of experimental measurements for fish with a non-inflated swimbladder.

The purpose of the present study was to estimate the *TS*–length relationships for four myctophid species (*Ceratoscopelus warmingii*, *Myctophum aspelum*, *Diaphus garmani*, and *D. chrysorhynchus*) that are abundant in temperate and subtropical waters of the Northwest Pacific. First we describe the morphological characteristics and growth of the swimbladder based on X-rays. Then, using morphological parameters of the swimbladders or fish body, theoretical sound-scattering models were applied to estimate the *TS* at 38 and 120 kHz, which are used commonly in scientific echosounders.

## Material and methods

Samples were obtained from five surveys conducted around southern Japan (36–25°N, 145–128°E) from August 2001 to June 2003 (Yasuma, 2004). Nine tows were carried out with an Isaacs–Kidd midwater trawl with codend mesh of 333 μm and five with a 4 $m^2$ MOCNESS with 2 mm mesh. Each tow was conducted at night, and the target layer was identified with an echosounder. The target sound-scattering layers were between 20 and 200 m deep. Hauling speeds were kept as slow as possible (0.1–0.5 m $s^{-1}$) to reduce the damage to the fish. Live fish were selected from the catch and kept for several hours in a tank on board to naturalize swimbladder condition, then placed in plastic bottles containing seawater and frozen rapidly (within 30 min.) to below –40°C. The effect of rapid freezing on swimbladder shape was considered to be negligible after preliminary experimentation (unpublished).

### Swimbladder measurement and allometry

In the laboratory, the bottles were thawed slowly in cold water over 24 h so the swimbladder shape would not change. In all, 123 *C. warmingii* (23–83 mm standard length), 93 *M. aspelum* (18–86 mm), 171 *D. garmani* (21–57 mm), and 85 *D. chrysorhynchus* (62–100 mm) were collected in this manner for swimbladder observation and *TS* estimation.

After external morphological measurements of the fish, a specialized "soft X-ray" imaging system (Softex PRO-TEST 100) was used to map the outlines of the swimbladders. All fish were X-rayed from lateral and dorsal sides, following Sawada *et al.* (1999), then dissected to confirm the shape of the swimbladder. The swimbladders of myctophids are thin-walled and gas-filled, atrophied without gas, and lack any structure (Butler and Pearcy, 1972; Yasuma *et al*., 2003). To estimate the acoustic scattering properties, we need to know the shape occupied by the gas. If there was no gas in the swimbladder, we treated the fish as a "swimbladderless" fish. If there was gas found, we treated the fish as a "swimbladdered" fish and mapped the shape occupied by the gas as the shape of the swimbladder. Outlines of the body shape of the swimbladderless fish were selected for subsequent *TS* model estimation using digital photo imagery. We measured swimbladder length $l_a$, swimbladder height $l_b$, and swimbladder width $l_c$ to the nearest 0.1 mm on outlines of the lateral and dorsal aspects. The main axis of the lateral image was used as swimbladder length. The swimbladder tilt angle was also measured using the outline of the lateral aspect (Figure 1).

Swimbladder volume $V_b$ was calculated from the formula of Capen (1967), i.e. $V_b = 4\pi/3(l_a/2)(l_b/2)(l_c/2)$, to estimate its contribution to whole-body volume, which was estimated by submersion in a graduated cylinder.

Organ growth usually follows simple allometric law (Huxley, 1932). Let $L$ be fish standard length, and $r$ the equivalent spherical radius of the swimbladder. Then the allometric relationship is $r = kL^q$, where $q$ is the allometric exponent (Saenger, 1989). Distinct types of swimbladder growth are associated with different ranges of $q$. We defined four types of growth: regressive growth ($q < 0$), negative allometric growth ($0 < q < 1$), isometric growth ($q = 1$), and positive allometric growth ($q > 1$). Introducing $x = \log(L)$ and $y = \log(r)$, allometric law can be expressed in the linear form $y = a + qx$, with $a = \log(k)$. The equivalent spherical radius $r$, given by $r = (l_a l_b l_c)^{1/3}$, can be used to observe trends in swimbladder growth because it can reduce the number of parameters. The effects of reducing parameters on swimbladder resonance scattering frequencies are negligible (<5%) when the proportions of the minor and the major axes (aspect

ratio) are relatively low ($l_b / l_a$ and $l_c / l_a > 0.3$), where the lower aspect (near spherical) is close to the value 1 (Stransberg, 1953; Andreeva, 1964).

### Sound-scattering model

The swimbladder is the main source of echoes in fish with swimbladders (Foote, 1980a; Ye and Farmer, 1996). Therefore, model calculations were applied to swimbladder shape in swimbladdered fish and for body shape in swimbladderless fish.

Based on morphological measurements of the swimbladder and body shape, we calculated theoretical values of *TS* related to fish pitch angle. According to Yasuma *et al.* (2003) and Yasuma (2004), we selected the vacant-PSM model (Furusawa, 1988) for swimbladdered fish and the liquid-DCM model (Ye, 1997; Ye *et al*., 1997) for swimbladderless fish, which matched the experimental *TS* measurements for the species we collected (Yasuma, 2004).

The PSM approximates a swimbladder by a simple spheroid using swimbladder length, height, and width. We followed the procedure of Sawada *et al.* (1999) and Yasuma *et al.* (2003) for PSM calculation. The main parameters, sound speed in seawater and in the swimbladder, were 1488 and 340 m $s^{-1}$, respectively. The sound speed in seawater was calculated using the equation of Mackenzie (1981) using the CTD data obtained while collecting the fish. Details of the PSM are described in Furusawa (1988).

The DCM describes a fish body as a series of adjacent, disc-like, cylindrical elements. We divided each outline into 20 equal parts, with 19 lines drawn perpendicular to the major axis, following Sawada *et al.* (1999) and Yasuma *et al.* (2003). Details of the DCM are described in Ye (1997) and Ye *et al.* (1997). The model requires the relative mass density ($g$) and the relative sound speed ($h$) of fish flesh against seawater. These parameters were measured previously using a density-bottle method (Greenlaw, 1977) and a time-average-approach method using a T-tube (Mikami *et al.*, 2000). Details of these measurements are described by Yasuma (2004) and Yasuma *et al.* (2006). Based on the temperature range of their main habitat (10–15°C), the values of $g$ and $h$ were 1.05 and 1.03 for *M. asperum*, and 1.01 and 1.03 for the other three species.

For both models, we calculated *TS* shifts with body pitch angle from –90° (head-down) to +90° (head-up) in 1° steps. Then, according to Foote (1980b), the averaged value of the *TS* calculated from a *TS* shift using the given pitch angle distribution was used as the *TS* of the fish. Here, we applied a distribution within a mean of 0° (horizontal direction) and a standard deviation of 15°.

It is convenient to normalize the *TS* value by the square of fish length. This is termed the reduced TS (*dB*) and given as $TS_{cm}$ when the fish length is in cm. The relationship between *TS* and fish standard length was summarized by the linear expression $y = mx + b$, where $y$ represents the value of *TS* (dB), and $x$ the log of standard length in cm. If the acoustic cross-section is proportional to length squared, the regression slope $m$ is assumed to be 20 when $TS_{cm}$ is represented by the intercept $b$ and takes a constant value over a range of sizes.

## Results

### Swimbladder morphology

Our samples included juvenile, immature, and mature *C. warmingii*, *M. aspelum*, and *D. garmani*, and immature and mature *D. chrysorhynchus*. Swimbladder length is plotted against

fish standard length in Figure 2. *C. warmingii*, *M. aspelum*, and *D. garmani* included swimbladdered and swimbladderless fish, but *D. chrysorhynchus* included only swimbladderless fish. In *C. warmingii*, the swimbladderless fish were small (23–43 mm), and there was an unformed swimbladder in each fish, seen under dissection. Swimbladdered fish were >33 mm, and all fish >44 mm had inflated swimbladders. In *M. asperum*, swimbladderless fish were separated out into two groups (18–33 mm, and 74–86 mm), and swimbladdered fish were of intermediate but overlapping length (31–77 mm). Fish in the smaller swimbladderless group had unformed swimbladders, and those in the larger group had visible swimbladders, but atrophied and without gas. Swimbladder length increased with growth under ~50 mm, but it decreased with growth over ~60 mm. In *D. garmani*, all fish <31 mm were swimbladderless, but >31 mm there were both swimbladderless and swimbladdered fish. Swimbladders of small fish (<30 mm) were unformed, bit in larger fish, swimbladders were visible even when categorized as swimbladderless fish, where the swimbladders were atrophied. All *D. chrysorhynchus* had atrophied swimbladders without gas.

The number of swimbladdered fish, the swimbladder aspect ratio (minor / major axis), the swimbladder tilt angle, and the percentage of swimbladder volume $V_b$ to the body volume are listed in Table 1. We defined the main axis of lateral images $l_a$ as the main axis, and the mean values of swimbladder height $l_b$ and swimbladder width $l_c$ as the minor axis in aspect ratio calculations. The highest aspect ratio was 0.3, and most fish had values from 0.5 to 1, in all four species. Smaller swimbladders have lower aspect ratios (closer to 1) and are nearly spherical, although the relationships between swimbladder length and aspect ratio were not significant. The $V_b$ percentage ranged from 0.01 to 2.63 and was <0.5 in most fish.

The relationship between the logarithmic scale of swimbladder equivalent radius and standard length is shown in Figure 3. The regression coefficient in each relationship represents the allometric exponent $q$. Values of $q$ were 1.3 in *C. warmingii* and 1.7 in *D. garmani*, implying that their swimbladders had positive allometric growth. We divided the swimbladder growth of *M. asperum* into two body length groups (<50 mm and >60 mm) because the plot of swimbladder length in Figure 2 implied different growth patterns. Allometric growth was positive ($q$ = 2.6) for the smaller group and regressive ($q$ = –1.7) for the larger group.

### *TS* estimation using theoretical models

Typical *TS* shifts of a swimbladdered and a swimbladderless fish estimated by the PSM and the DCM models are shown as a function of fish pitch angle in Figure 4. The *TS* shifts of swimbladdered fish estimated by the PSM are smooth at 38 and 120 kHz, suggesting a relatively small effect of fish orientation. On the other hand, the *TS* shifts of swimbladderless fish estimated by the DCM model show relatively narrow and pronounced peaks at 38 and 120 kHz, suggesting that changes in fish orientation would have a major effect on *TS* variance. The results showed that those effects were more pronounced in large fish at high frequencies.

The relationship between estimated tilt-averaged *TS* and the log of the standard length (cm) of swimbladdered fish is shown in Figure 5. The equations of the linear regression in Figure 5 and the ranges of $TS_{cm}$ are listed in Table 2. In *C. warmingii* and *D. garmani*, the regression slope $m$ was >20 at both frequencies. This suggests that the acoustic cross-section is not proportional to the square of body length and that the *TS* increases faster than body length. In *M. asperum*, the *TS* increased significantly faster than body length ($m$ > 35) in the small size class (31–48 mm), but it *TS* decreased with body length in the large size class (61–77 mm), indicating

regressive allometric growth of the swimbladder in that species (Figure 5, Table 2). No major differences between the *TS* value at 38 kHz and 120 kHz were seen in any swimbladdered fish (ANCOVA, $p > 0.05$).

The relationship between the tilt-averaged *TS* and the log of standard length (cm) of swimbladderless fish is shown in Figure 6. The equations of the linear regression shown in Figure 6 and the ranges of $TS_{cm}$ are listed in Table 3. We selected 25 each of *C. warmingii* and *D. chrysorhynchus*, and 50 each of *M. asperum* and *D. garmani* from the entire length range of swimbladderless fish. $TS_{cm}$ values were much lower in swimbladderless than in swimbladdered fish. The regression slope *m* was high (>30) at 38 kHz in each species, suggesting that the increase in *TS* is faster than that of body length. On the other hand, the regression slope was <20 at 120 kHz in each species, suggesting that the increase in *TS* is slower than that of body length.

## Discussion

### Potential diel differences in swimbladder shape

All our fish samples were captured relatively shallow (<200 m) at night. Many myctophids undertake diel vertical migration, and this might lead to a diel difference in swimbladder volume (Kanwisher and Ebeling, 1957). However, acoustic studies of deep-water fish suggest that they maintain a constant volume or a constant mass of gas in their swimbladders during vertical migration (Vent and Pickwell, 1977; Benoit-Bird *et al*., 2003). A constant gas volume is needed to maintain neutral buoyancy, and many mesopelagic fish achieve this through gas exchange (D'Aoust, 1971; Suetsugu and Ohta, 2004). This suggests that swimbladder shape does not change unless there are artefact effects, e.g. rapid pressure changes caused by fast towing. Our samples were free of these effects because the sampling gear was towed as slowly as possible and live fish were selected for the swimbladder observations.

### Swimbladder morphology in acoustic perspective

The *C. warmingii*, *M. asperum*, and *D garmani* had inflated swimbladders at some period of their life. Although the swimbladder shape varied with species and life stage, they had common features different from other families of fish. The swimbladder length of common pelagic fish is about one-third of the standard length, swimbladder volume is from 4 to 10% of body volume, the aspect ratios range from 0.1 to 0.3, and the tilt angle is about 5 or 6° (Capen, 1967; Furusawa, 1989). On the other hand, the swimbladder volumes of the species investigated here were <0.5% of body volume in most fish, implying that the values of $TS_{cm}$ would be lower than that of other pelagic species. Moreover, most swimbladdered fish had short bodies and egg-shaped (i.e. low aspect ratio) swimbladders, showing a relatively broad distribution of the tilt angle (Table 1). Wider tilt angle distributions may introduce biases for pitch-averaged values of *TS* estimated by the theoretical model. However, that effect would be negligible at 38 or 120 kHz, because the swimbladder lengths of the current species were too small to detect a measurable change in *TS* with pitch angle (Yasuma, 2004).

Unformed swimbladders were observed in juvenile *C. warmingii*, *M asuperum*, and *D. garmani* (Figure 2). The swimbladder of many fish species becomes physoclistous at some point in its early life history, and gas secretion does not occur until then (Powers, 1932). Our results reveal the timing of first gas production in three species (Figure 2, Table 2), likely important information because the value of *TS* changes critically in the presence of gas. We have no

information on juvenile *D. chrysorhynchus*, but it is possible that they too have a gas-containing swimbladder early in life, though further observation is necessary to confirm this.

All swimbladdered species showed positive allometric growth after the onset of gas secretion into the swimbladder, but in *D. garmani*, both swimbladdered and swimbladderless specimens were observed over a broad range of body lengths. Further, larger *M. asperum* showed regressive growth, and mature fish were mainly swimbladderless. The co-occurrence of swimbladdered and swimbladderless fish in a single species, in this case *D. garmani*, has been reported for other myctophids, e.g. *Diaphus theta* and *Symbolophorus californiensis* (Butler and Pearcy, 1972; Neighbors and Nafpaktitis, 1982). The relative growth rate (body length vs. swimbladder length) varies in many fish species (Kitajima *et al*., 1985; Sadayasu, 2005). However, regressive growth or atrophy of the swimbladder is specific to myctophids and a few other mesopelagic fish (Marshall, 1971; Saenger, 1989).

Although the causes of these unique features are unclear, diel vertical migration is thought to be one of the major triggers. An inflated swimbladder would be unfavourable for fish migrating vertically, because the maintenance of a constant swimbladder volume throughout their vertical range would require considerable gas secretion and resorption. Therefore, their conditions may reflect species-dependent or ontogenetic changes in migratory behaviour. Many mesopelagic fish that either lack or have a small swimbladder retain their buoyancy by increasing lipid content (Marshall, 1960; Butler and Pearcy, 1972; Neighbors and Nafpaktitis, 1982).

## Reliability of model estimation

Yasuma (2004) compared theoretical estimates with experimental measurements using examples of the same species and confirmed that each fish showed similar patterns of *TS* shift between theoretical (represented in Figure 4) and experimental results. The reliability of our theoretical estimations is supported by this observation. However, if the fish undergo a steep orientation in the field, the averaged *TS*, which applies the stated value of pitch-angle distribution, would have potential error, especially for swimbladderless fish. There is little information about the swimming behaviour (orientation) of myctophids. Barham (1970) observed it using a diving camera and reported that many fish have a nearly vertical orientation at night, although most are orientated in the almost horizontal by day. The pitch-angle distributions of myctophids are still unknown, so direct visual observations with a video camera are required to estimate the *TS* more precisely.

## *TS* of swimbladdered fish and the potential effect of acoustic resonance

McClatchie *et al*. (2003) stated that deep-water fish such as macrourids and oreosomatids have small swimbladders and low values of *TS*. They also noted that the *TS* of these deep-water fish did not follow the 20 log *L* relationship, because the swimbladder cross-section grew rapidly in relation to fish length. The $TS_{cm}$ values of other swimbladdered fish, such as gadoids and clupeoids, range from –65 to –72 dB (MacLennan and Simmonds, 1992). However, our results show that many swimbladdered fish have a low $TS_{cm}$ (<–75 dB), suggesting a lower *TS* in proportion to body length (Table 2). Additionally, the *TS* values of the species we examined did not follow the 20 log *L* relationship and increased rapidly in relation to body size (Figure 5, Table 2). These results support the suggestion of McClatchie *et al*. (2003) and underscore the importance of information on species-specific swimbladder condition and its growth for

development of theoretical estimation of *TS*. There are very few reports about the *TS* regression in fish such as *M. asperum* (Figure 5), but atrophy of the inflated swimbladder occurs in many myctophids and they may have potential *TS* regression (Butler and Pearcy, 1972; Neighbors and Nafpaktitis, 1982; Saenger, 1989; Neighbors, 1992; Yasuma *et al*., 2003).

Acoustic backscatter from the swimbladder increases the effect of resonance when the swimbladder is small, in relation to acoustic wavelength (e.g., $kr << 1$, where $k$ is the wavenumber and $r$ the equivalent spherical radius of the gas field), and this effect becomes larger in deeper water (Capen, 1967; Love, 1978). As described above, the swimbladder size of the four species examined here is small, and these species occupy relatively deep layers, so the effect of swimbladder resonance should be considered. The acoustic backscatter cross-section ($\sigma$) at 38 and 120 kHz, computed by the resonance model (Love, 1978), was normalized by the square of equivalent spherical radius $r^2$, and plotted in relation to the equivalent spherical radius in Figure 7. Peaks of each line are the point of resonance at each depth, and the effect of resonance is negligible where the equivalent radius is sufficiently large and the $\sigma / r^2$ takes an asymptotic value. At 38 kHz, the resonance would be negligible shallower than 300 m if the equivalent radius is >1 mm. However, there would be an effect of resonance deeper than 300 m if the equivalent radius is <1 mm. At 120 kHz, the resonance is negligible shallower than 300 m if the equivalent radius is >0.5 mm. Figure 8 shows the relationship between the equivalent radius of the swimbladder (log) and fish standard length, as obtained here. Among swimbladdered fish, small *C. warmingii* (<55 mm), small *M. asperum* (<40 mm), and all size classes of *D. garmani* contained many fish with small swimbladders (<1 mm). This suggests that they would be under the effect of resonance at a depth of 300 m (or even at 100 m) at 38 kHz. Myctophid fish live in relatively deep water, and the use of low frequencies (e.g. 38 kHz), when there is less absorption, may be appropriate to the field biomass survey. However, if the target fish school consists mainly of small fish, adequate ways of measurement, including the use of high frequencies (e.g. 120 kHz) and the use of data collected at night when the schools ascend, should be considered to preclude any effect of resonance. In contrast, differences in *TS* values (at 38 vs. at 120 kHz) under the effect of resonance may be helpful to other analyses, such as for school detection.

### *TS* of swimbladderless fish

Using 11 swimbladderless species of myctophid, Yasuma (2004) determined the values of tilt-averaged *TS* at four frequencies (38, 70, 120, and 200 kHz) obtained by experimental measurement and the DCM model, and summarized the $TS_{cm}$ values as a function of $L/\lambda$, where $\lambda$ is the wavelength (Figure 9). According to that analysis, values of $TS_{cm}$ increase rapidly until $L/\lambda$ approaches ~2 (~7.8 cm at 38 kHz, and ~2.5 cm at 120 kHz), and then becomes asymptotic, with little fluctuation. Most swimbladderless specimens of the present species had low values of $L/\lambda$ (<2) at 38 kHz, which is why the coefficients of the *TS*–length relationships were well above 20 and the *TS* increased rapidly with body growth (Figure 6, Table 3). On the other hand, the $L/\lambda$ values of most fish were >2 at 120 kHz, where $TS_{cm}$ vary about asymptotic values.

Although there is little information about the *TS* of swimbladderless fish (Foote, 1980a; McClatchie and Ye, 2000), Foote (1980a) reported that the $TS_{cm}$ of a swimbladderless pelagic fish ranged from –90 to –80 dB when $L/\lambda$ was greater than 2. This is similar to our results, although some *M. asperum*, which have a notably larger body density, had higher values of *TS*. *TS* values of smaller fish (<7.8 cm) would be lower at 38 kHz than at 120 kHz. This may be

helpful for detecting schools in the field, if the target school consists mainly of such smaller fish.

### Complexity of the *TS*–length relationship caused by a biphasic swimbladder condition

The *TS*–length equations listed in Tables 2 and 3 are proposed for use in analyses of field data, and they provide a lot of information needed for understanding the ecological structure of the deep-scattering layer in the Northwest Pacific. However, *C. warmingii*, *M. asperum*, and *D. garmani* have overlaps between swimbladdered and swimbladderless fish at certain size ranges (Figure 2, Tables 2 and 3), and this causes an intricacy in determining the *TS* of a fish in these size ranges. Especially for *D. garmani*, the overlap is over a wide size range from juvenile to mature, and this may preclude reliable estimation of biomass. Similar overlaps have been found in other myctophid species, such as *Myctophum aurolaternatum*, *Diaphus theta*, and *Symbolophorus californiensis* (Capen, 1967; Butler and Pearcy, 1972; Neighbors, 1992). Neighbors (1992) found different conditions of the swimbladder in a similar size class of *S. californiensis* and suggested that the difference was attributable to the depth of capture. Butler and Pearcy (1972) also found a biphasic swimbladder condition in *S. californiensis* and suggested the possibility of regional, seasonal, or sex-related differences. We collected our samples under different environmental conditions and divided them based only on species and body size. Therefore, we do not know what environmental factors contribute to the biphasic swimbladder condition. Further work may, however, allow us to evaluate swimbladder condition and determine a better *TS*–length equation, by typifying the swimbladder condition against other variables such as season of the year, sampling site, sampling depth, or sampling time.

## Acknowledgements

We thank the captains and crews of the RV “Hakuho Maru”, the RV “Tansei Maru”, and the RV “Wakataka Maru” for their cooperation in fish sampling. The work was supported by a grant from the Fisheries Research Agency of Japan, and a Grant-in-aid for Scientific Research (No. 14560142) from the Japan Society for the Promotion of Science.

## References

Andreeva, I. B. 1964. Scattering of sound by air bladders of fish in deep sound-scattering ocean layers. Soviet Physics Acoustics, 10: 17–20.

Barham, E. G. 1970. Deep-sea fish. Lethargy and vertical orientation. *In* Biological Sound Scattering in the Ocean (preliminary edn), pp. 100–118. Ed. by B. Farquhared. Maury Center for Ocean Science, Report 5, Washington DC.

Benoit-Bird, K. J., Au, W. W. L., Kelley, C. D., and Taylor, C. 2003. Acoustic backscattering by deepwater fishes measured *in situ* from a manned submersible. Deep-Sea Resarch I, 50: 221–229.

Butler, J. L., and Pearcy, W. J. 1972. Swimbladder morphology and specific gravity of myctophids off Oregon. Journal of the Fisheries Research Board of Canada, 29: 1145–1150.

Capen, R. L. 1967. Swimbladder morphology of some mesopelagic fishes in relation to sound scattering. Naval Electron Laboratory Report, 1447, San Diego, CA.

D'Aoust, B. G. 1971. Physiological constraints of vertical migration by mesopelagic fishes. *In* Proceedings of an International Symposium on Biological Sound Scattering in the Ocean, pp. 86–97. Ed. by G. B. Farquhar. Department of the Navy, Washington DC.

Foote, K. G. 1979. Fish target-strength-to-length regressions for application in fisheries research. In Proceedings of the Ultrasonic International 19, Graz, Austria, pp. 327–333.

Foote, K. G. 1980a. Importance of the swimbladder in acoustic scattering by fish: a comparison of gadoid and mackerel target strength. Journal of the Acoustical Society of America, 67: 2084–2089.

Foote, K. G. 1980b. Averaging of fish target strength functions. Journal of the Acoustical Society of America, 67: 504–515.

Furusawa, M. 1988. Prolate spheroidal models for predicting general trends of fish target strength. Journal of the Acoustical Society of Japan, 9: 13–24.

Furusawa, M. 1989. Bubbles and underwater sounds – swimbladder and sound scattering by fish. Journal of the Marine Acoustical Society of Japan, 16: 181–196.

Greenlaw, C. F. 1977. Backscattering spectra of preserved zooplankton. Journal of the Acoustical Society of America, 62: 44–52.

Gjøsaeter, J., and Kawaguchi, K. 1980. A review of the world resources of mesopelagic fish. FAO Fisheries Technical Paper, 193. 151 pp.

Horne, J. K., and Clay, C. S. 1998. Sonar systems and aquatic organisms: matching equipment and model parameters. ICES Journal of Marine Science. 55: 1296–1306.

Huxley, J. S. 1972. Problems of Relative Growth,, 2nd edn. Dover, New York. 312 pp.

Kanwisher, J., and Ebeling, A. 1957. Composition of the swim-bladder gas in bathypelagic fishes. Deep-Sea Research, 4: 211–217.

Kitajima, C., Tsukashima, Y., and Tanaka, M. 1985. The voluminal changes of swimbladder of larval red-sea bream *Pagrus major*. Bulletin of the Japanese Society of Scientific Fisheries, 51: 759–764.

Love, R. H. 1978. Resonant acoustic scattering by swim-bladder-bearing fish. Journal of the Acoustical Society of America, 64: 571–580.

Mackenzie, K. V. 1981. Nine-term equation for sound speed in the oceans. Journal of the Acoustical Society of America, 70: 807–812.

MacLennan, D. N., and Simmonds, E. J. 1992. Fisheries Acoustics. Chapman and Hall, London.

Marshall, N. B. 1960. Swimbladder structure of deep-sea fishes in relation to their systematics and biology. Discovery Reports, 31: 1–222.

Marshall, N. B. 1971. Swimbladder development and the life of deep-sea fishes. *In* Proceedings of an International Symposium on Biological Sound Scattering in the Ocean, pp. 69–73. Ed. by G. B. Farquhar. Department of the Navy, Washington DC.

McClatchie, S., Macaulay, G. J., and Coombs, R. 2003. A requiem for the use of 20 $\log_{10}$ Length for acoustic target strength with special reference to deep-sea fishes. ICES Journal of Marine Science, 60: 419–428.

McClatchie, S., and Ye, Z. 2000. Target strength of an oily deep-water fish, orange roughy (*Hoplostethus atlanticus*). 2. Modeling. Journal of the Acoustical Society of America, 107: 1280–1285.

Mikami, N., Mukai, K., and Iida, K. 2000. Measurements of density and sound speed contrasts for estimating krill target strength using theoretical scattering models. Nippon Suisan Gakkaishi, 66: 682–689.

Neighbors, M. A. 1992. Occurrence of inflated swimbladders in five species of lanternfishes (family Myctophidae) from waters off southern California. Marine Biology, 114: 355–363.

Neighbors, M. A., and Nafpaktitis, B. G. 1982. Lipid compositions, water contents, swimbladder

morphologies and buoyancies of nineteen species of midwater fishes (18 myctophids and 1 neoscopelid). Marine Biology, 66: 207–215.

Powers, E. B. 1932. The relation of respiration of fishes to environment. Ecological Monographs, 11: 385–473.

Sadayasu, K. 2005. Study on precise estimation of fish target strength. PhD dissertation, Hokkaido University. 290 pp. (in Japanese).

Saenger, A. R. 1989. Bivariate normal swimbladder size allometry models and allometric exponents for 38 mesopelagic swimbladdered fish species commonly found in the north Sargasso Sea. Canadian Journal of Fisheries and Aquatic Sciences, 46: 1986–2002.

Sawada, K., Ye, Z., Kieser, R., and Furusawa, M. 1999. Target strength measurements and modeling of walleye pollock and Pacific hake. Fisheries Science, 65: 193–205.

Strasberg, M. 1953. The pulsation frequency of non-spherical gas bubbles in liquids. Journal of the Acoustical Society of America, 25: 536–537.

Suetsugu, K., and Ohta, S. 2004. Functional change in the swimbladder with fish size in *Coryphaenoides acrolepis*. Deep-Sea Research I, 51: 1275–1282.

Vent, R. J., and Pickwell, G. V. 1977. Acoustic volume scattering measurements with related biological and chemical observations in the northeastern tropical Pacific. *In* Oceanic Sound Scattering Prediction, pp. 697–716. Ed. by N. R. Andersen, and B. J. Zahuranec. Plenum Press, New York.

Yasuma, H. 2004. Studies of the acoustical biomass estimation of myctophid fishes. PhD dissertation, University of Tokyo. 237 pp. (in Japanese).

Yasuma, H., Sawada, K., Ohshima, T., Miyashita K., and Aoki, I. 2003. Target strength of mesopelagic lanternfishes (family Myctophidae) based on swimbladder morphology. ICES Journal of Marine Science, 60: 584–591.

Yasuma, H., Takao, Y., Sawada, K., Miyashita, K., and Aoki, I. 2006. Target strength of the lanternfish, *Stenobrachius leucopsarus* (family Myctophidae), a fish without an airbladder, measured in the Bering Sea. ICES Journal of Marine Science, 63: 683–692.

Ye, Z. 1997. A novel approach to sound scattering by cylinders of finite length. Journal of the Acoustical Society of America, 102: 877–884.

Ye, Z., and Farmer, D. M. 1997. Acoustic scattering by fish in the forward direction. ICES Journal of Marine Science, 53: 249–252.

Ye, Z., Hoskinson, E., Dewey, R. K., Ding, L., and Farmer, D. M. 1997. A method for acoustic scattering by slender bodies. Journal of the Acoustical Society of America, 102: 1964–1976.

## Figure legends

**Figure 1**. Morphometry on lateral and dorsal swimbladder X-ray images. The symbols $l_a$, $l_b$, and $l_c$ represent swimbladder length, swimbladder height, and swimbladder width, respectively.
**Figure 2**. Plots of swimbladder length of (a) *Ceratoscopelus warmingii*, (b) *Myctophum asperum*, (c) *Diaphus garmani*, and (d) *Diaphus chrysorhynchus*, against fish standard length.
**Figure 3**. Relationship between logarithmic scale of the swimbladder equivalent radius $r$ and standard length $L$ of (a) *C. warmingii*, (b) *M. asperum*, and (c) *D. garmani*. Regression lines and equations are shown. The $\beta$ (in brackets) indicates 95% confidence limits of the regression line.
**Figure 4**. Examples of the theoretical *TS* shift of a swimbladdered (left panel) and a swimbladderless (right panel) fish, as a function of fish pitch angle. Positive angles are head-up and negative angles head-down. The bold and dotted lines denote the *TS* at 38 kHz and 120 kHz, respectively. The left panel shows the *TS* of a *C. warmingii* (standard length 60 mm; swimbladder length 9.1 mm; aspect ratio 0.45), the right panel the *TS* of a *D. chrysorhynchus*

(standard length 74 mm).
**Figure 5**. Plots of target strength against log of standard length (in cm) for swimbladdered (a) *C. warmingii*, (b) *M. asperum*, and (c) *D. garmani*, (left column) at 38 kHz, and (right column) at 120 kHz.
**Figure 6**. Plots of target strength against log of standard length (cm) for swimbladderless (a) *C. warmingii*, (b) *M. asperum*, (c) *D. garmani*, and (d) *D. chrysorhynchus*, (left column) at 38 kHz, and (right column) at 120 kHz.
**Figure 7**. Normalized acoustic backscatter cross-section $\sigma / r^2$ at depths of 0, 50, 100, and 300 m computed by Love (1978) as functions of $r$ at 38 kHz (top panel) and 120 kHz (lower panel).
**Figure 8**. Log of the swimbladder equivalent spherical radius of (a) *C. warmingii*, (b) *M. asperum*, and (c) *D. garmani* as a function of fish standard length. The dotted, solid, dashed, and dotted-dashed lines indicate 3, 2, 1, and 0.5 mm, respectively.
**Figure 9**. Plot of $TS_{cm}$ of swimbladderless myctophids as a function of $L/\lambda$, after Yasuma (2004).

## Running headings

*H. Yasuma* et al.
*Swimbladdder condition and target strength of myctophids*

**Table 1**. Ranges of swimbladder aspect ratio, swimbladder tilt angle, and percentage of swimbladder volume $V_b$ in body volume (mean ± *s.d.*).

| Species | *n* | Aspect ratio | Tilt angle (°) | $V_b$ percentage (%) |
|---|---|---|---|---|
| *Ceratoscopelus warmingii* | 83 | 0.28 – 0.97 (0.61 ± 0.22) | 0.0 – 24.8 (14.9 ± 9.9) | 0.01 – 2.63 (0.49 ± 0.50) |
| *Myctophum asperum* | 43 | 0.32 – 1.00 (0.75 ± 0.19) | 0.0 – 21.8 (10.6 ± 8.7) | 0.01 – 1.48 (0.39 ± 0.37) |
| *Diaphus garmani* | 82 | 0.27 – 1.00 (0.57 ± 0.23) | 0.0 – 19.7 (8.7 ± 7.2) | 0.01 – 1.53 (0.38 ± 0.37) |

**Table 2**. Equations of the linear regressions plotted in Figure 5 and the ranges of standard length. The *y*-values represent *TS* (dB), and the *x*-values the log of the standard length (cm). $\beta$ indicates the 95% confidence limits of the regression slope *m*. Ranges of $TS_{cm}$ at each length range are also shown.

| Species | Length range (mm) | *n* | Frequency (kHz) | $y = mx + b$ | | | | $TS_{cm}$ range (dB) |
|---|---|---|---|---|---|---|---|---|
| | | | | *m* | *b* | $R^2$ | $\pm\beta$ | |
| *Ceratoscopelus warmingii* | 33 – 83 | 81 | 38 | 26.3 | –78.1 | 0.30 | 9.1 | –82.3 to –67.7 |
| | | | 120 | 26.1 | –79.2 | 0.31 | 8.7 | –82.6 to –68.6 |
| *Myctophum asperum* | 31 – 48 | 31 | 38 | 45.4 | –88.6 | 0.45 | 15.9 | –79.9 to –68.8 |
| | | | 120 | 36.3 | –84.6 | 0.44 | 12.6 | –80.2 to –69.7 |
| | 61 – 77 | 8 | 38 | –135.2 | –57.3 | 0.69 | 80.1 | –87.2 to –69.8 |
| | | | 120 | –130.8 | –52.4 | 0.67 | 82.5 | –87.6 to –70.4 |
| *Diaphus garmani* | 31 – 57 | 75 | 38 | 34.5 | –83.5 | 0.46 | 8.1 | –81.7 to –68.7 |
| | | | 120 | 32.7 | –83.3 | 0.49 | 7.6 | –82.6 to –69.4 |

**Table 3**. Equations of the linear regressions plotted in Figure 6 and the ranges of standard length. The *y*-values represent *TS* (dB), and the *x*-values the log of the standard length (cm). $\beta$ indicates the 95% confidence limits of the regression slope *m*. Ranges (and average) of $TS_{cm}$ at each length range are also shown.

| Species | Length range (mm) | *n* | Frequency (kHz) | $y = mx + b$ | | | | $TS_{cm}$ range (dB) and (average) |
|---|---|---|---|---|---|---|---|---|
| | | | | ***m*** | ***b*** | $R^2$ | $\pm\beta$ | |
| *Ceratoscopelus warmingii* | 23 – 43 | 25 | 38 | 49.4 | –112.2 | 0.93 | 6.0 | –103.9 to –92.1 (–96.7) |
| | | | 120 | 10.4 | –82.6 | 0.45 | 5.0 | –90.6 to –86.1 (–87.6) |
| *Myctophum asperum* | 18 – 33 | 50 | 38 | 52.7 | –108.3 | 0.98 | 2.3 | –100.5 to –75.9 (–90.4) |
| | 74 – 86 | | 120 | 17.9 | –80.9 | 0.85 | 1.9 | –85.0 to –77.1 (–82.1) |
| *Diaphus garmani* | 21 – 53 | 50 | 38 | 54.0 | –113.5 | 0.94 | 4.2 | –105.2 to –86.9 (–94.4) |
| | | | 120 | 6.9 | –8.4 | 0.34 | 3.0 | –92.5 to –85.5 (–88.8) |
| *Diaphus chrysorhynchus* | 62 – 100 | 25 | 38 | 30.5 | –96.3 | 0.81 | 5.8 | –88.2 to –85.3 (–86.9) |
| | | | 120 | –9.1 | –63.2 | 0.24 | 8.5 | –92.3 to –87.5 (–89.2) |

Fig. 1

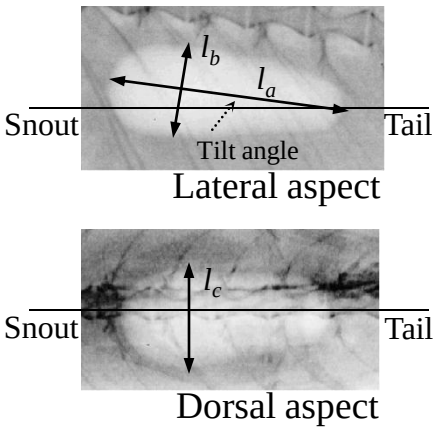
$l_b$
$l_a$
Snout
Tail
Tilt angle
Lateral aspect
$l_c$
Snout
Tail
Dorsal aspect

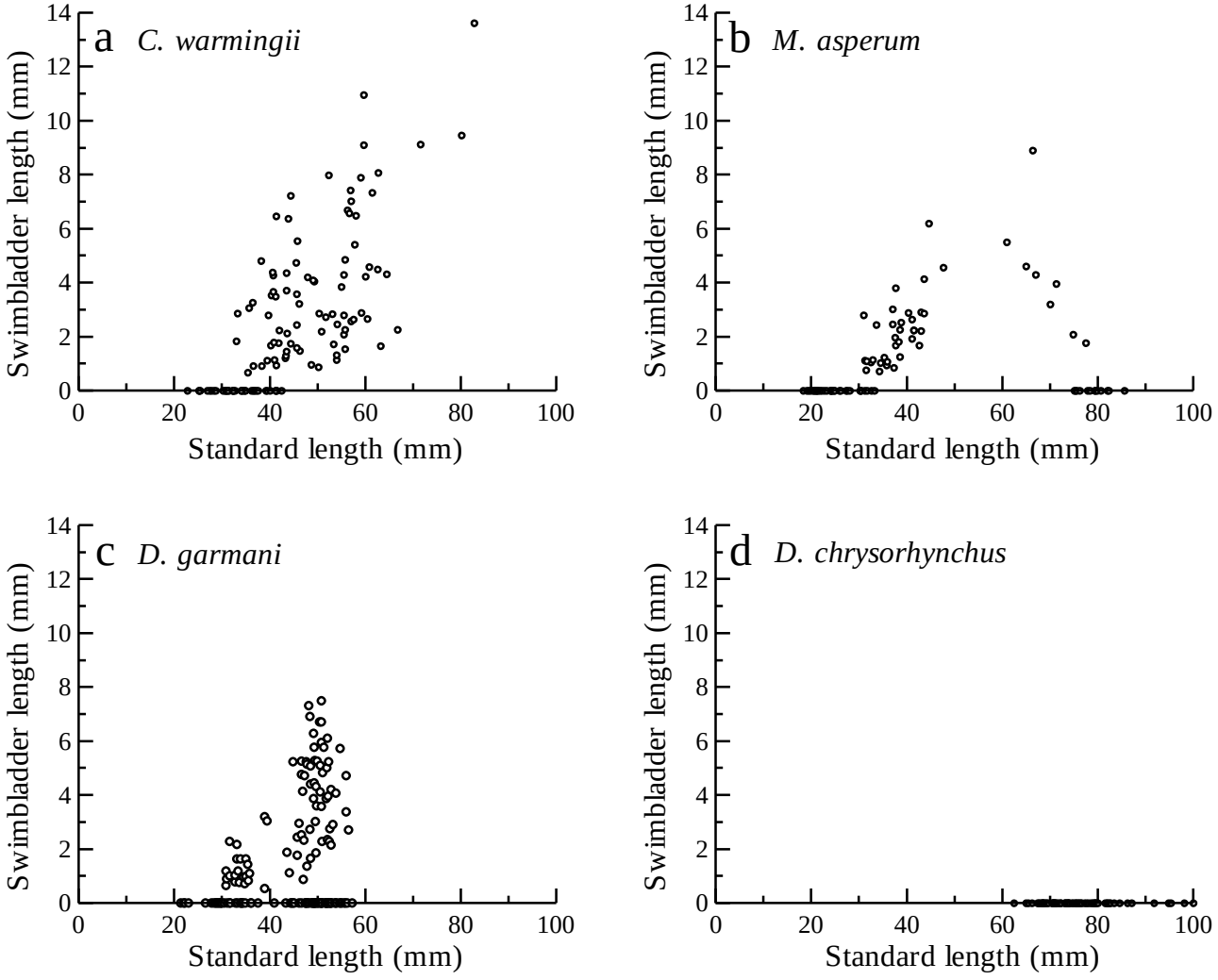
a C. warmingii
b M. asperum
c D. garmani
d D. chrysorhynchus
Swimbladder length (mm)
Standard length (mm)
0
2
4
6
8
10
12
14
0
20
40
60
80
100

Fig. 3

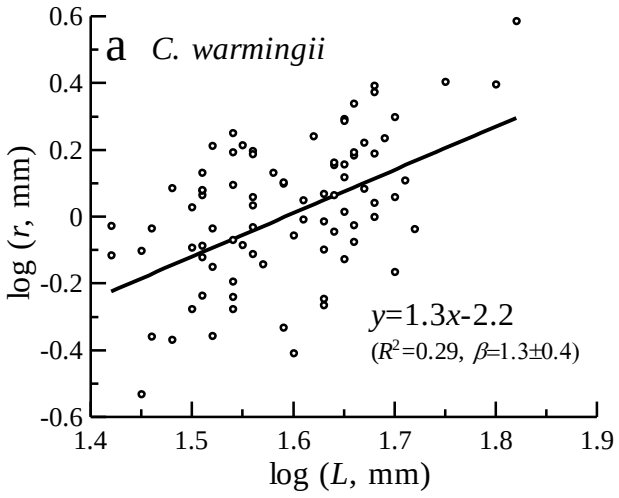
a C. warmingii
y=1.3x-2.2
(R²=0.29, β=1.3±0.4)
log (r, mm)
log (L, mm)
0.6
0.4
0.2
0
-0.2
-0.4
-0.6
1.4
1.5
1.6
1.7
1.8
1.9

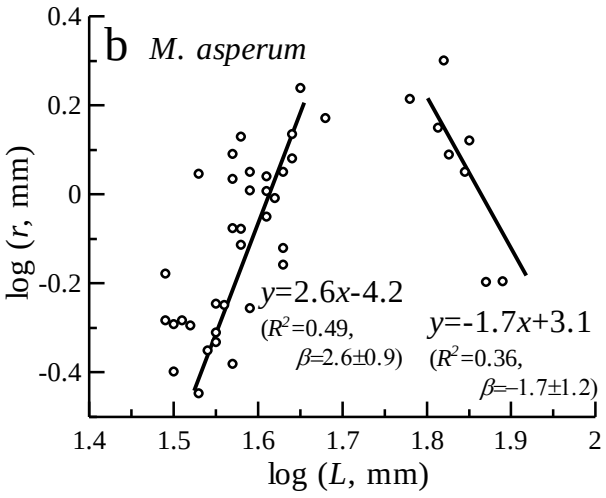
b M. asperum
y=2.6x-4.2
(R²=0.49,
β=2.6±0.9)
y=-1.7x+3.1
(R²=0.36,
β=–1.7±1.2)
log (r, mm)
log (L, mm)
0.4
0.2
0
-0.2
-0.4
1.4
1.5
1.6
1.7
1.8
1.9
2

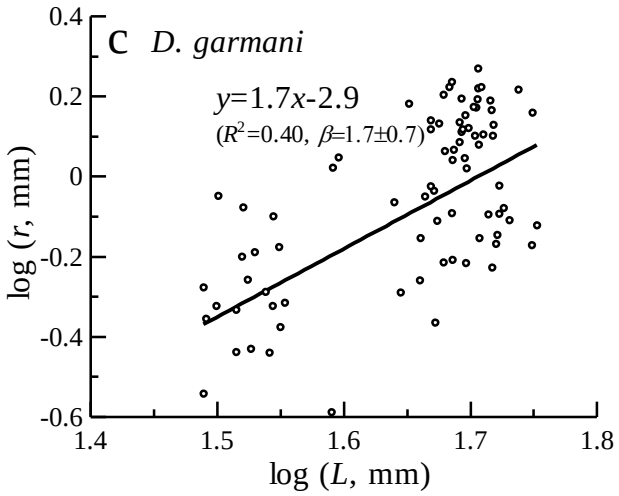
c D. garmani
y=1.7x-2.9
(R²=0.40, β=1.7±0.7)
log (r, mm)
log (L, mm)
0.4
0.2
0
-0.2
-0.4
-0.6
1.4
1.5
1.6
1.7
1.8

Fig. 4

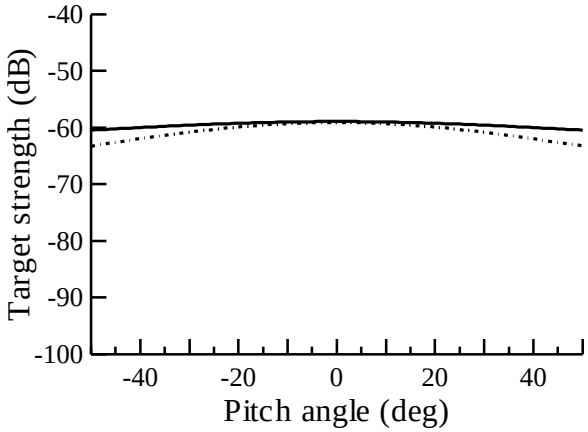
-40
-50
-60
-70
-80
-90
-100
Target strength (dB)
-40
-20
0
20
40
Pitch angle (deg)

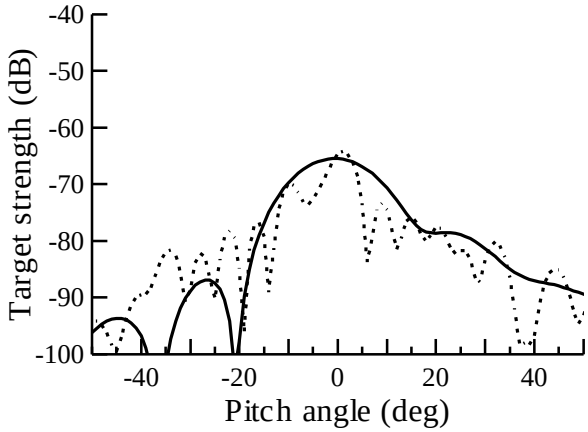
-40
-50
-60
-70
-80
-90
-100
Target strength (dB)
-40
-20
0
20
40
Pitch angle (deg)

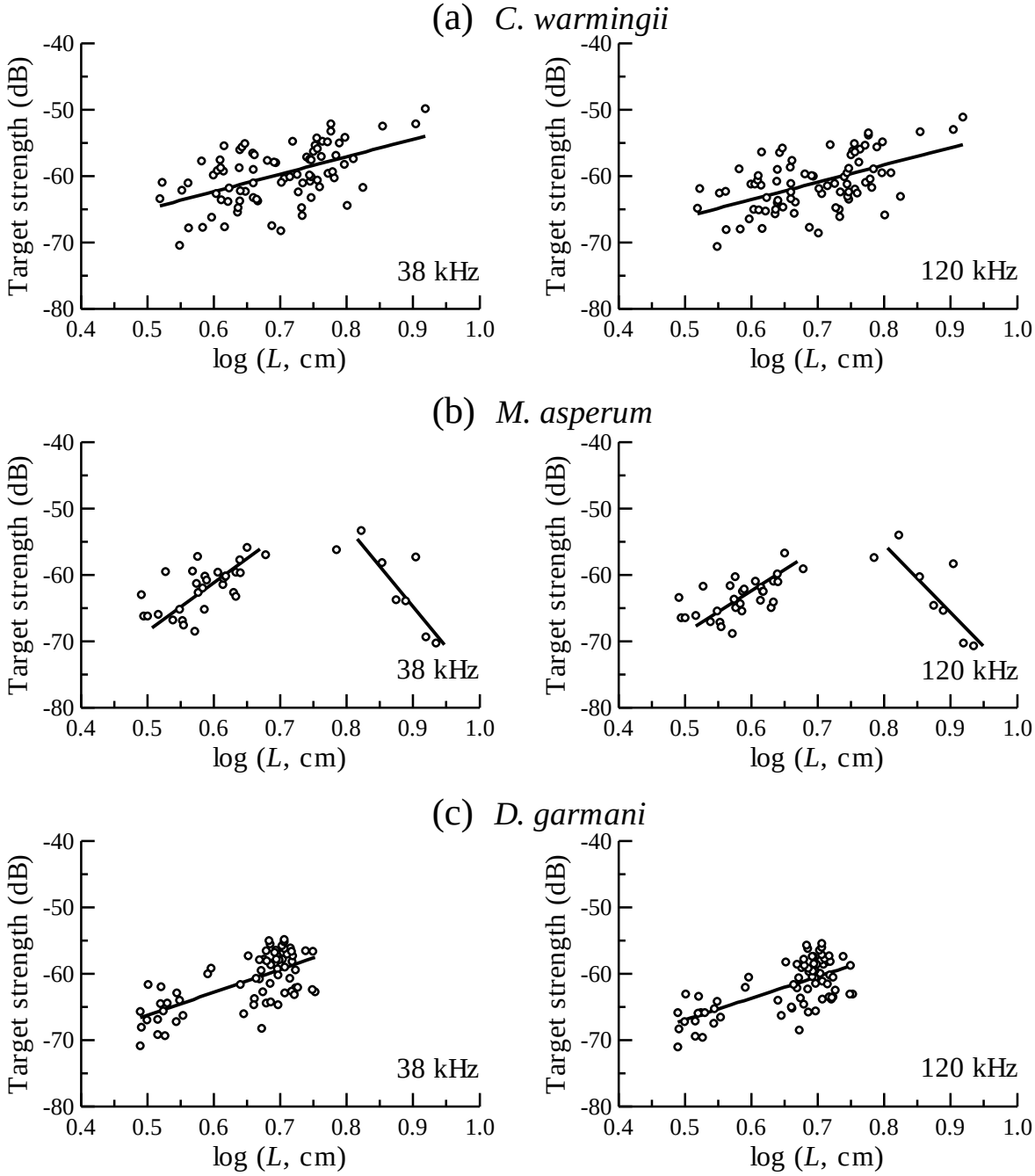
(a) C. warmingii
Target strength (dB)
-40
-50
-60
-70
-80
0.4
0.5
0.6
0.7
0.8
0.9
1.0
log (L, cm)
38 kHz
120 kHz
(b) M. asperum
38 kHz
120 kHz
(c) D. garmani
38 kHz
120 kHz

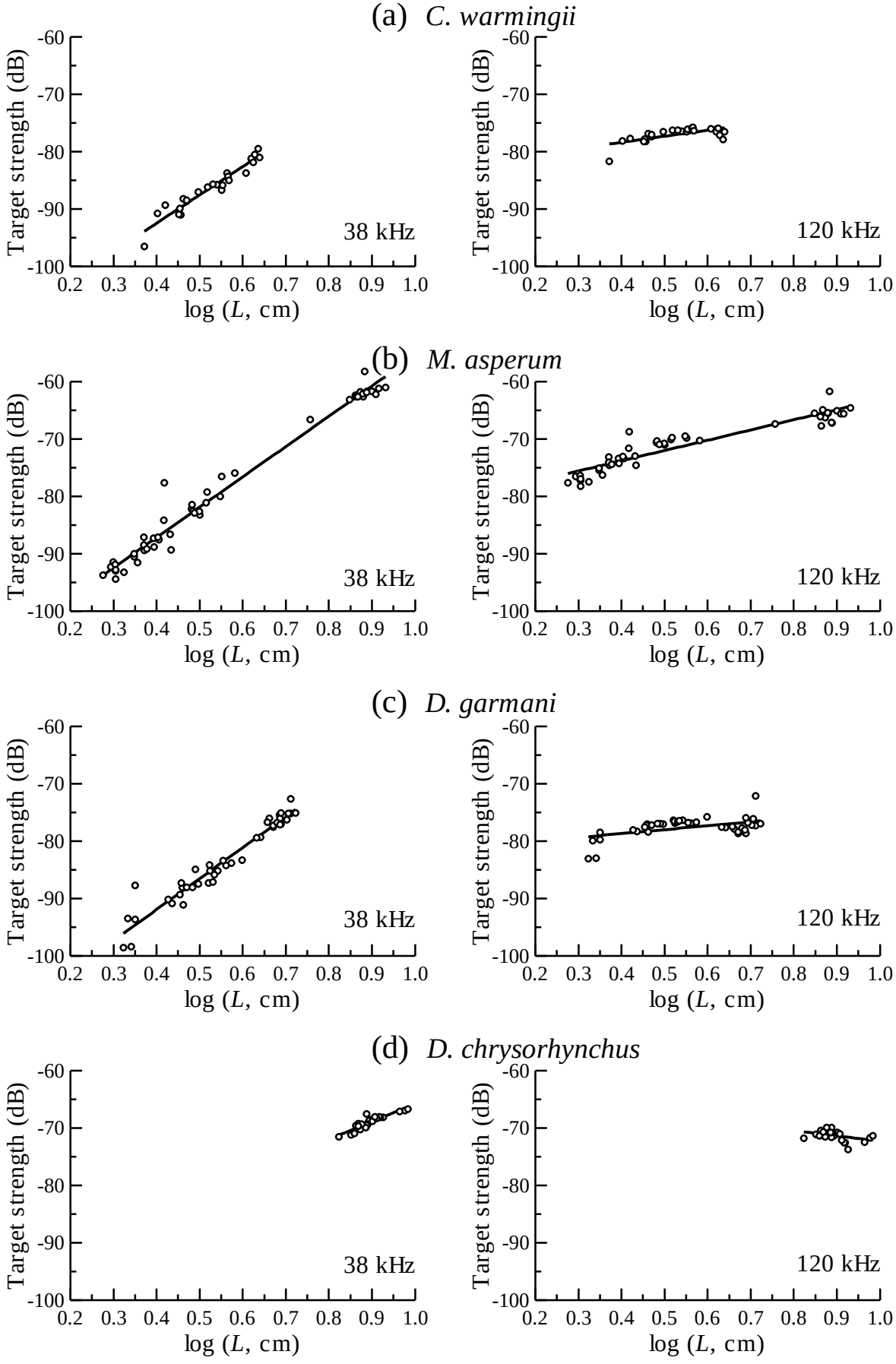
(a) C. warmingii
(b) M. asperum
(c) D. garmani
(d) D. chrysorhynchus
Target strength (dB)
log (L, cm)
38 kHz
120 kHz
-60
-70
-80
-90
-100
0.2
0.3
0.4
0.5
0.6
0.7
0.8
0.9
1.0

Fig. 7

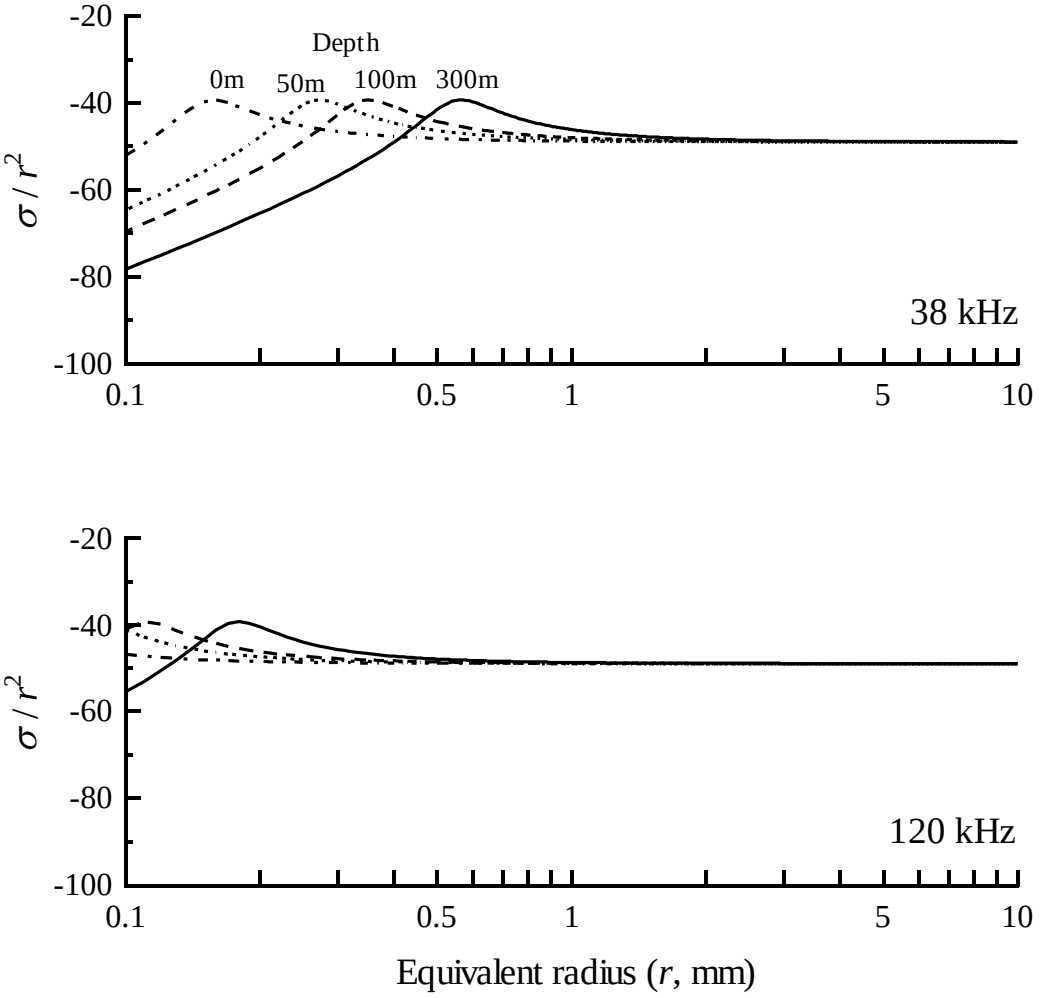
-20
-40
-60
-80
-100
σ / r2
Depth
0m
50m
100m
300m
38 kHz
0.1
0.5
1
5
10
-20
-40
-60
-80
-100
σ / r2
120 kHz
0.1
0.5
1
5
10
Equivalent radius (r, mm)

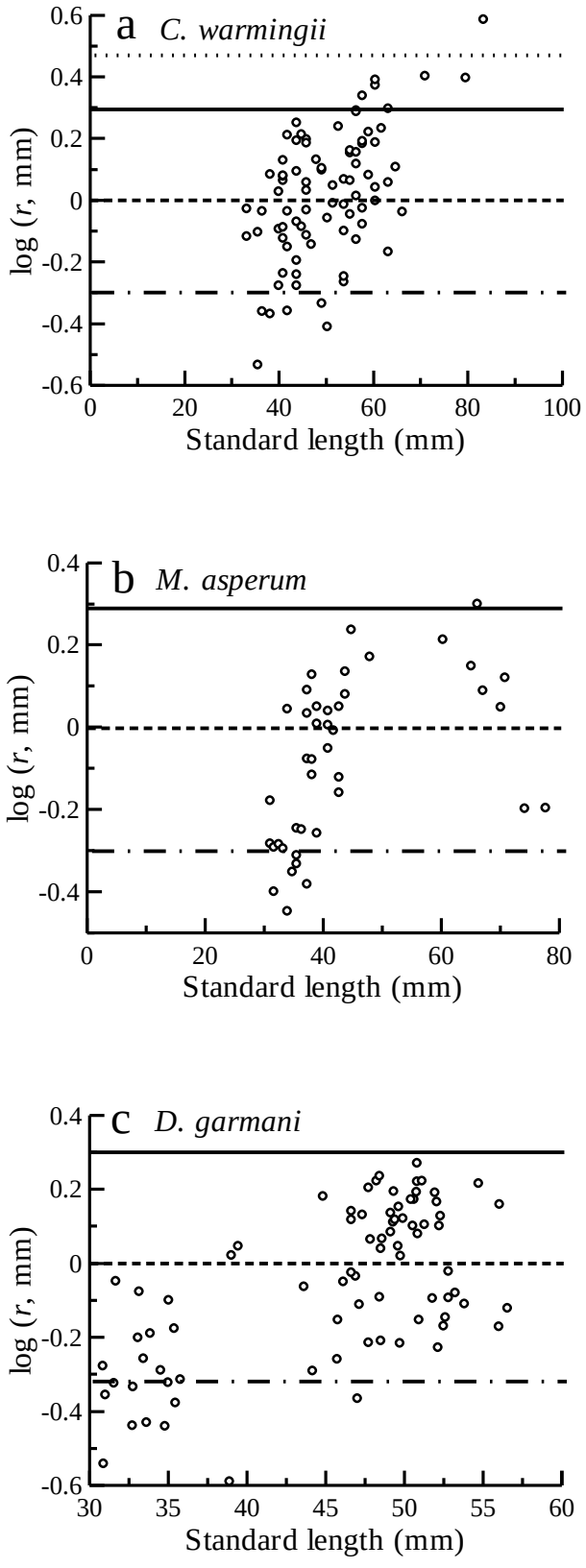
a C. warmingii
log (r, mm)
Standard length (mm)
b M. asperum
log (r, mm)
Standard length (mm)
c D. garmani
log (r, mm)
Standard length (mm)

Fig. 9